

# Parameter affecting the I<sup>3</sup>S algorithm reliability: how does correcting for body curvature affect individual recognition?

Giacomo Rosa <sup>A</sup>, Fanny Guillaud<sup>A</sup>, Pauline Priol<sup>B</sup> and Julien Renet<sup>A,C</sup>

<sup>A</sup>Conservatoire d'espaces naturels de Provence-Alpes-Côte d'Azur, Pôle Biodiversité Régionale, Appartement n°5, 96 Rue Droite, 04200 Sisteron, France.

<sup>B</sup>StatiPop Scientific Consulting, 4 Avenue de Nîmes, 34190 Ganges, France.

<sup>C</sup>Corresponding author. Email: [julien.renet@cen-paca.org](mailto:julien.renet@cen-paca.org)

## Abstract

**Context.** In recent years, multiple computer algorithms, which allow us to perform photographic capture–recapture analysis, have been developed. Their massive application, also in wildlife demographic and ecological studies, is largely due to the fact that these tools are non-invasive and non-expensive. To maximise the performance of these programs, it is essential to have a good photo-standardisation so as to avoid bias in the results. A lot of ‘non-standardised’ photos are not usable for capture–mark–recapture (CMR) analysis, entailing the loss of potentially exploitable data.

**Aims.** No study has accurately investigated the effect of the corporal bending of an animal on the performance of the interactive individual identification system (I<sup>3</sup>S) algorithm. For this reason, we assessed the effect of this photographic standardisation parameter (PSP) on the reliability of this algorithm.

**Methods.** We assessed the effect of the body position of *Triturus cristatus* between capture and recapture photos on the error rates of a group of standardised pictures, performing a generalised linear model analysis. We have also evaluated the effect of image correction (i.e. straightening of newts’ bodies) on the error rates (expressed by false rejection rates, FRRs) of the first (standardised) photo-group (G1) and of a non-standardised photo-group (G2). To perform this, we used I<sup>3</sup>S-Pattern<sup>+</sup> for the photo-matching analysis and I<sup>3</sup>S-Straighten for the correction of the pictures.

**Key results.** The difference of body angles between capture and recapture pictures had a significantly increased error rates in G1. Digital correction of body bending reduced the error rates. For the pictures where corporal bending was not digitally corrected, the top 20 FRRs were 0.38 and 0.33 for G1 and G2 respectively. For corrected (straightened) pictures, the top 20 FRRs were 0.026 and 0.15.

**Conclusions.** Our findings showed a high impact of newt corporal bending and photographic treatment on the I<sup>3</sup>S algorithm reliability.

**Implications.** We provide some recommendations to avoid or minimise the effects of this PSP and improve photo-standardisation during and after CMR studies of species of Urodela. In this way, pictures that would be unusable in photo-matching software under current practice could become usable, increasing the available data to conduct a survey.

**Additional keywords:** corporal bending, false rejection rate, I<sup>3</sup>S-Pattern<sup>+</sup>, I<sup>3</sup>S-Straighten, photographic standardisation, *Triturus cristatus*.

Received 11 December 2019, accepted 9 June 2020, published online 8 September 2020

## Introduction

Digital photo-identification methods in capture–mark–recapture (CMR) studies are widely employed (Ferner 2010) and their application is constantly growing, because they are less expensive and less invasive than are other individual marking techniques (such as e.g. toe clipping, PIT tags). The individual visual comparison (or visual matching), seen as a laborious and unreliable method with a large dataset (Cruickshank and Schmidt 2017), has given way to photo-matching algorithms, such as, for example, interactive individual identification system (I<sup>3</sup>S; Van Tienhoven *et al.* 2007), speeded-up robust features (SURF; Bay *et al.* 2008) and scale-invariant feature transform (SIFT;

Bolger *et al.* 2012), which allow fast and reliable individual recognition. I<sup>3</sup>S is one of the most used algorithms for wildlife monitoring, owing to its free availability, efficiency and reliability.

The I<sup>3</sup>S algorithm has been embedded in several software interfaces (I<sup>3</sup>S Classic, Spot, Contour, Pattern and Pattern<sup>+</sup>) particularly adapted for surveys of a variety of vertebrate taxa, such as, for example, reptiles (Sreekar *et al.* 2013; Dunbar *et al.* 2014; Araujo *et al.* 2016; Treilibs *et al.* 2016; Hayes *et al.* 2017; Steinmetz *et al.* 2018; Suriyamongkol and Mali 2018; Wessels *et al.* 2018), amphibians (Ribero and Rebelo 2011; Sannolo *et al.* 2016; Davis *et al.* 2018; Matos *et al.* 2018) and fishes (Van Tienhoven *et al.* 2007; Chaves *et al.* 2016; Araujo *et al.* 2017).

Species that can be individually identified with this method must satisfy certain requirements. In particular, they have to show some morphological or colouring features (such as e.g. colour body pattern for fish or amphibian species, arrangement and shape of the scales in reptile species). Obviously, it is necessary to respect certain conditions of picture standardisation to ensure reliability and avoid misidentification, which could affect the estimation of demographic parameters (Morrison *et al.* 2016). Picture resolution, view angle, lack of body curve, depth of field and lighting condition (e.g. avoiding glare with the flash) are some of the conditions required in standardised pictures (Sacchi *et al.* 2016; Matthé *et al.* 2017). Among these, the bending of the body is a serious issue because the I<sup>3</sup>S algorithm basically assumes that an animal is rigid and in two dimensions. For this reason, I<sup>3</sup>S-Straighten (I<sup>3</sup>S-S) has been developed (Den Hartog and Reijns 2015) to straighten the picture (i.e. the photographed subject) and, consequently, the body bending, so as to improve the photo-matching performance of the I<sup>3</sup>S algorithm.

However, we did not find any reference that accurately assesses the effect of body curvature and the correction of this photographic standardisation parameter (PSP) on the reliability of the I<sup>3</sup>S algorithm. For this reason, we used a partially standardised photo-group of *Triturus cristatus* to evaluate the effect of newt body curvature on I<sup>3</sup>S algorithm reliability (i.e. false rejection rate values) between capture and recapture photos. We also assessed the effect of the correction of the body curvature (i.e. partially automated straightening of newt bodies) on the error rates of the first group and a non-standardised photo-group. The results provided some technical suggestions that could improve photographic standardisation for monitoring species of Urodela.

## Materials and methods

### Model photo-matching program and species

To assess the reliability of I<sup>3</sup>S algorithm we used I<sup>3</sup>S-Pattern<sup>+</sup> (I<sup>3</sup>S-P<sup>+</sup>; Den Hartog and Reijns 2016), an improved version (available for free from [http://www.reijns.com/i3s/download/I3S\\_download.html](http://www.reijns.com/i3s/download/I3S_download.html), accessed 2 July 2020) of I<sup>3</sup>S-Pattern developed for coping better with variation in colour intensity, shape of body pattern (e.g. spot) and light conditions (e.g. low light, reflection of camera flash).

For other versions of the I<sup>3</sup>S package, the proposed approach is a partially automated digital identification (PADI) system (i.e. each picture is pre-processed by the user) that relies on natural marks to identify individual animals (Van Tienhoven *et al.* 2007). Unlike the other versions, where the user manually annotates the location and or the size of the spots, Pattern and Pattern<sup>+</sup> automatically extract them using the SURF algorithm (Bay *et al.* 2008).

The I<sup>3</sup>S-P<sup>+</sup> software essentially reduces the picture to two values, i.e. background and foreground, or pattern and not pattern. It is most effective for monitoring amphibians that have a high-contrast coloration pattern (e.g. *B. variegata*, *T. cristatus*; Den Hartog and Reijns 2016).

We used pictures of adult great crested newt, *Triturus cristatus*, from two monitored populations in south-eastern France whose identity was determined beforehand by visual matching. The great crested newt has an irregular ventral spot pattern that is unique for each individual, making this species a

good model to test this software family (Sannolo *et al.* 2016). All individuals were captured with Ortmann funnel traps (Drechsler *et al.* 2010) and a dip net. They were released immediately after photography at the exact location of capture. Capture permits for this program were issued by order of the Prefect (2014-252-0001, 2019-s-05), according to French law.

### Process of assessing I<sup>3</sup>S algorithm reliability

We created a first I<sup>3</sup>S-P<sup>+</sup> database including two photo-groups (G1 and G2) of 150 individuals each.

The pictures included in G1 were taken with a standardised method, namely, during the day, with a Nikon D90 (2248 × 4288; sensor: CMOS 12.2 Mpx), equipped with a zoom Nikon 28–105 mm (1 : 3.5–4.5 D), without any light source, and with a fixed distance between the camera and the subject (40 cm). All individuals were maintained upside down with a glass plate and photographed perpendicularly on the ventral face by a single observer. Corporal bending was not corrected during the photo shoot. We selected the pictures of the most curved newts, cropped to a resolution of 1024 × 1400.

Group G2 was a heterogeneous photo group that contained non-standardised images. Pictures were taken during the night, always by using a light source (flash or headlight) and without keeping a fixed distance between the camera and the subject. Pictures were taken with different cameras having different resolutions, namely, Canon Powershot S110 (pixel resolution 4000 × 3000), Canon EOS 1000D (3888 × 2592), equipped with a zoom Canon 35–105 mm (1 : 3.5–4.5), Olympus TG-610 (2048 × 1536), Panasonic DMC-FT5 (4608 × 3456), SONY DSC-TX5 (3648 × 2736) and Nikon COOLPIX S6800 (4608 × 3456). A field assistant held individual animals against the glass so as to correct their body curvature. Ventral pictures were taken perpendicularly with a camera placed on the other side of the glass.

Therefore, these two opposite photo groups represent an extreme situation, concerning the photo-standardisation, in which one set contains only the best pictures possible, whereas the other contains the worst.

Every picture was integrated after defining three reference points (on both sides of the neck and at the base of the cloaca) and the area of interest. We plotted between 35 and 45 key points, which were found to be the best range for the analysis on I<sup>3</sup>S-P (Sannolo *et al.* 2016).

After creating the picture database, we processed in the same way 39 pictures of recaptured individuals present in G1 and 39 pictures present in G2, corresponding to 78 different individuals (i.e. 78 pictures of recaptured individuals were compared with the database of 300 individuals). We excluded multiple captures for the same newt to avoid a simplification of the algorithmic analysis on some individuals and a positive influence on the error rate (Matthé *et al.* 2017). Also, the recapture pictures were not embedded after each analysis with I<sup>3</sup>S-P<sup>+</sup>, but were deleted to avoid increasing the size of the picture database and affecting the error rate (Bolger *et al.* 2012).

The I<sup>3</sup>S-P<sup>+</sup> software offers up to 100 ‘top-ranked’ matches following a decreasing calculated score provided by its algorithms. Then, the user has to search visually for the correct individual among the software proposal. We annotated the ranks of the

recaptures up to 50 and selected the best high-scoring matches (HSMs), namely, Top1, Top5, Top10 and Top20. Corresponding error rates were reported in terms of false rejection rate (FRR), which reflects the failure of software to match two pictures of the same individual (Jain 2007). The FRR is given by the ratio between the number of false rejections and the total number of identification attempts and its value runs from 0 (best) to 1 (worst) (Sacchi *et al.* 2016).

#### Assessment of body-curve effects on error rates (FRRs)

So as to evaluate the effect of the different positions of newt bodies on the error rate, we analysed the difference in angles ( $\delta$ ) between the pictures of the 39 captures and the corresponding recaptures within G1. To generate this measure, we used the software MB Ruler 5.3 and the formula  $\delta = X^{\circ}_{CAP} - X^{\circ}_{RECAP}$ , or conversely. We utilised as reference points the base of cloaca and the tip of the snout, following the axis of the body (Fig. 1).

This analysis was performed using pictures only from G1, because the dataset of G2 was too heterogeneous and contained too many variables (e.g. glare, variable distance). Thus, we could compare only the angle differences between the two groups. The characterisation of these differences showed that G1 (s.d.  $\pm 14.02$ , min = 15, max = 60, mean = 17.7) had bigger angle differences than did G2 (s.d.  $\pm 4.05$ , min = 0, max = 3, mean = 5.5).

#### Assessment of newt body straightening on error rates (FRRs)

We evaluated this effect on each group independently. Even if G2 shows heterogeneous photos, including a strong variability of the PSPs, we thought it was important to assess the algorithmic performance of I<sup>3</sup>S-P<sup>+</sup> after straightening the photos in this group.

We utilised I<sup>3</sup>S Straighten ver. 1.0 (I<sup>3</sup>S-S; Den Hartog and Reijns 2015), a version that allows correction of body curvature in a two-dimensional plane, straightening and cropping the picture

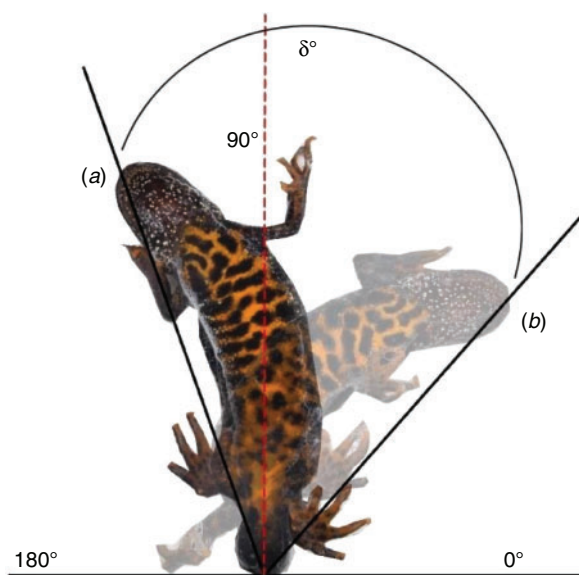


**Fig. 1.** Procedure to measure the difference in newt body angle (i.e. the delta) between (a) capture and (b) recapture photos.

where the newts are curved and not in a standardised position (i.e. straight). In this way, we digitally corrected the capture (300) and recapture pictures (78) of the two groups, turning all the angles in right angles of 90° (straight position; Fig. 1). In this way, we can consider the photos of each group as ‘untreated’ or ‘treated’.

A new I<sup>3</sup>S-P<sup>+</sup> database was created with treated photos and the inclusion of the recaptures followed the same process as performed above.

#### Statistical analysis

First, we assessed the effect of delta angle (i.e. the difference of body angles between capture and recapture pictures) on the rank of the untreated pictures of G1. Second, we evaluated the effect of the correction of the corporal bending (i.e. straightening with I<sup>3</sup>S-S) for the standardised group (G1) by comparing untreated and treated photos. Then we assessed the same process for the non-standardised group (G2) in another GLM.

So as to achieve this, three generalised linear models (GLMs) were created (Glonek and McCullagh 1995). Ranks (i.e. FRR) and delta angle are positive discrete variables and data follow a Poisson distribution (Gardner *et al.* 1995). Each GLM has a link function that makes the model linear; the link function of Poisson regression is a logarithmic function (Ver Hoef and Boveng 2007). Poisson GLMs can be written as

$$\log(Y_i) = a \times x_i + b,$$

where  $Y$  is the variable to be explained,  $b$  is the intercept,  $a$  is the effect of variable or factor  $x_i$ ,  $a$  and  $b$  are estimated by the GLM.

For each GLM, tests of goodness of fit (GoF) verify how well the model fits the data. The dispersion parameter and Pseudo- $R^2$  are calculated for the GoF. To test whether the over- or under-dispersion was significant, the function ‘pchisq’ (chi-square test) was used. The null deviance must follow a chi-square distribution, with the null hypothesis of ‘the over- or under-dispersion is not statistically significant’.

For models with significant over- or under-dispersion, we used quasi-Poisson and negative binomial GLMs, which are Poisson regression forms with a new parameter to take under and over dispersion into account. The GoF analysis described above was then repeated.

All analyses were performed in the software R.3.6.0 with the interface RStudio (R Development Core Team 2018). Functions ‘glm’, ‘glm.nb’ and ‘pchisq’ belong to packages ‘MASS’ (Venables and Ripley 2002) and ‘stats’ (Chambers and Hastie 1992).

## Results

*Does the difference of the newt’s position between capture and recapture affect the error rates of G1?*

Dispersion parameters for all Poisson GLMs were much higher than 1, suggesting a poor fit of these models to the data. For this reason, we used a negative binomial regression for every test.

The analysis showed that the delta angles have a statistically significant ( $P < 0.01$ ) positive effect on the rank for the untreated photo in G1 (Analysis I in Table 1). The larger the delta angle is, the greater the rank (Fig. 2). The model explained

**Table 1. Generalised linear model analysis**

Analysis I, assessment if ranks vary with delta body angles for untreated pictures in Group G1; Analysis II, assessment if ranks depend on photo treatment in Group G1; Analysis III, assessment if ranks depend on photo treatment in Group G2

Analysis	Parameter	Estimation	s.e.	P	Dispersion parameter ( $\phi$ )	Pseudo- $R^2$
I	Intercept	2.22173	0.33399	<0.001	1.1973	0.15
	Delta	0.04390	0.01471	<0.010	$P = 0.19$	
II	Intercept	1.3471	0.2997	<0.001	1.11	0.29
	Untreated photos	1.8061	0.4109	<0.001	$P = 0.24$	
III	Intercept	1.9994	0.2479	<0.001	1.16	0.08
	Untreated photos	0.9369	0.0.3471	<0.010	$P = 0.16$	

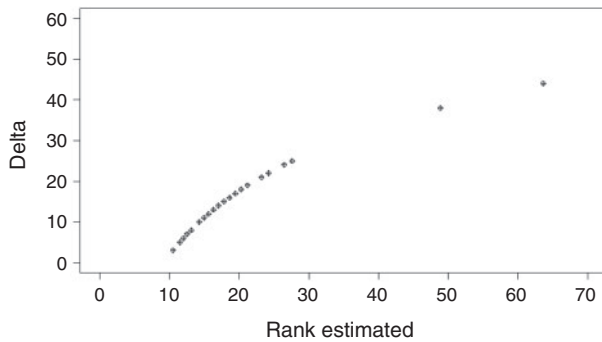


**Fig. 2.** Scatter plot of delta angle as a function of rank estimated for Group G1.

15% of data and was adjusted to the data; the over-dispersion was not significant.

*Does the image treatment with I<sup>3</sup>S-S significantly improve the algorithmic performance of I<sup>3</sup>S, starting with a group of standardised (G1) and non-standardised (G2) photos?*

The second GLM, using data from photos in G1, showed that the ranks of the untreated photos were 1.8061 times greater than were the ranks of the treated photos, with a significant  $P$ -value ( $P < 0.001$ ). This model was adjusted to the data and explained 29% of it (Analysis II in Table 1).

In the third GLM, using data from photos in G2, the ranks of the untreated photos were 0.9369 times greater than were the ranks of the treated photos. The results were statistically significant ( $P < 0.01$ ), but the model explained only 8% of data (Analysis III in Table 1).

In terms of FRRs, the untreated photos showed high values for the four HSMs (Top1 to Top20) and, for the two groups, they were between 0.72 (G1, Top1) for the worst value, and 0.33 (G2, Top20) for the best value (Table 2). The Group G2 always gave better results than did Group G1 for the four HSMs.

In a similar analysis performed with the treated (I<sup>3</sup>S-S) photos, FRRs were much lower for both G1 and G2 (Table 2). The values were between 0.44 (G2, Top1) for the worst value, and 0.026 (G1, Top20) for the best value. In this case, G1 showed lower FRRs than did G2 for all four HSMs.

**Table 2. Comparison of false rejection rates (FRRs) between the two photo groups (G1 and G2), before and after a treatment with an interactive individual identification system (I<sup>3</sup>S-Straighten software, see text)**

High-scoring match	Untreated		Treated (I <sup>3</sup> S-S)	
	G1	G2	G1	G2
Top1	0.718	0.436	0.282	0.436
Top5	0.462	0.385	0.154	0.282
Top10	0.410	0.359	0.077	0.179
Top20	0.385	0.333	0.026	0.154

**Discussion**

*Impact of corporal bending and I<sup>3</sup>S-S treatment on I<sup>3</sup>S algorithm reliability*

Our findings indicated (1) a strong negative impact of the angle generated by newt corporal bending on the algorithmic performance of I<sup>3</sup>S, (2) a low reliability (large FRRs) of the I<sup>3</sup>S algorithm (from I<sup>3</sup>S-P<sup>+</sup>) with untreated or non-standardised pictures of the groups, which can be significantly improved with a pre-processing approach (I<sup>3</sup>S-S). That bending may increase error has been already hypothesised by the authors of the I3S software suite, who encouraged maximal standardisation of photos.

The generated error rates (FRRs) were generally high. The best results were in Top20, with a matching of 61.5% for G1 and 66.7% for G2, indicating that I<sup>3</sup>S-P<sup>+</sup> is quite unreliable in matching non-standardised pictures. Group G2 showed better FRRs than did Group G1, despite a worst standardisation of the shooting. A probable explanation for this may be that the pictures of newts in G1 were more curved than those in G2 (owing to the manual straightening of the operators; see Materials and methods).

The I<sup>3</sup>S-S treatment leads to the opposite situation and confirms the strong effect of delta angle on the FRR. Indeed, G1 showed very low FRRs values, particularly in Top20 and Top10, with a matching of 97.4% and 92.3% respectively. These values are substantially higher than those observed by Matthé et al. (2017; e.g. Top10 = 84.5%; FRR: 0.155). This is probably due to the fact that G2 contained pictures that had been taken with different resolutions (use of several cameras), with the cameras being placed at a variable distance from the subject. More specifically, the photo size was substantially smaller because of the cropping performed by I<sup>3</sup>S-S on the body zone

of interest (i.e. ventral side). Depending on the distance between the camera and the newt, cropping induces a decrease, more or less important, of picture quality, which could, in turn, affect also the reliability of the algorithm. This loss of pixel resolution was not noticeable for G1 because the pictures of this group had been cropped previously and taken with a standardised method, keeping a short distance from the newts. All these elements suggest an effect, which is probably not irrelevant, of picture resolution on error rates from G2. In the same way as Treilibs *et al.* (2016), we suspect that flash reflection on wet skin played also a substantial role in the self-matching scores of G2. However, in the presence of multiple PSPs within this heterogeneous group, it was not possible to evaluate the incidence of each of them (including the body curvature) on the error rates achieved with I<sup>3</sup>S-P+. The influence of other parameters (in addition to the body curvature) is probably not negligible as shown by the results of the GLM for G2, where the model explained only 8% of data (Analysis III in Table 1). These elements highlight, once again, the importance of maximising the photographic standardisation (i.e. picture size and resolution, view angle, depth of field and lighting condition, among other things) during photo shooting.

#### Management implications

The results of the present study allow us to propose some recommendations to improve photo-standardisation during monitoring of Urodela species. Above all, it is fundamental to maintain the animal as straight as possible during the shooting session, as already remarked by other authors (e.g. Den Hartog and Reijns 2015; Sacchi *et al.* 2016; Matthé *et al.* 2017).

However, we showed that attempts to manually correct body curvature (G2) were not conclusive. Moreover, a prolonged handling of the newts could eventually cause lesions and transmit pathogens. Consequently, it would be ideal to keep the amphibian as straight as possible, placing it on its back with a sheet of glass on the ventral side. The operator should then straighten the pictures with a pre-processing tool, such as I<sup>3</sup>S-S, at a later time. Second, it is essential to always keep a fixed and short distance between the camera and the subject to avoid loss of picture resolution after manual or automated cropping. Third, the same camera model should be used to take all pictures in a particular project, so as to maintain constant picture sizes and resolutions. Finally, it is advisable to not use any light source (e.g. flash or headlamp) when taking photos, so as to avoid a glaring effect. Consequently, it could be better to conduct the monitoring session in daylight while avoiding direct sunlight.

#### Conflicts of interest

The authors declare no conflicts of interest.

#### Acknowledgements

We warmly thank Jurgen den Hartog, Renate Reijns (I<sup>3</sup>S team) and Professor Sebastiano Salvidio (Genoa University) for providing useful comments and Dr Nigel Taylor (Tour du Valat, Research Institute for the Conservation of Mediterranean Wetlands) for his valuable help in improving the English language. We also thank all volunteers for assistance in the field. Two anonymous referees helped us improve an earlier version of the manuscript. This research did not receive any specific funding.

#### References

- Araujo, G., Montgomery, J., Pahang, K., Labaja, J., Murray, R., and Ponzio, A. (2016). Using minimally invasive techniques to determine green sea turtle *Chelonia mydas* life-history parameters. *Journal of Experimental Marine Biology and Ecology* **483**, 25–30. doi:10.1016/j.jembe.2016.06.004
- Araujo, G., Snow, S., So, C. L., Labaja, J., Murray, R., Colucci, A., and Ponzio, A. (2017). Population structure, residency patterns and movements of whale sharks in southern Leyte, Philippines: results from dedicated photo-ID and citizen science. *Aquatic Conservation* **27**(1), 237–252. doi:10.1002/aqc.2636
- Bay, H., Ess, A., Tuytelaars, T., and Van Gool, L. (2008). Speeded-up robust features (SURF). *Computer Vision and Image Understanding* **110**(3), 346–359. doi:10.1016/j.cviu.2007.09.014
- Bolger, D. T., Morrison, T. A., Vance, B., Lee, D., and Farid, H. (2012). A computer-assisted system for photographic mark-recapture analysis. *Ecology and Evolution* **3**, 813–822. doi:10.1111/j.2041-210X.2012.00212.x
- Chambers, J. M., and Hastie, T. (1992). ‘Statistical Models in S.’ (Wadsworth & Brooks/Cole Advanced Books & Software: Pacific Grove, CA, USA.)
- Chaves, L. C. T., Hall, J., Feitosa, J. L. L., and Côté, I. M. (2016). Photo-identification as a simple tool for studying invasive lionfish *Pterois volitans* populations. *Journal of Fish Biology* **88**(2), 800–804. doi:10.1111/jfb.12857
- Cruikshank, S. S., and Schmidt, B. R. (2017). Error rates and variation between observers are reduced with the use of photographic matching software for capture-recapture studies. *Amphibia-Reptilia* **38**, 315–325. doi:10.1163/15685381-00003112
- Davis, C. L., Teitsworth, E. W., and Miller, D. A. W. (2018). Combining data sources to understand drivers of spotted salamander (*Ambystoma maculatum*) population abundance. *Journal of Herpetology* **52**(2), 116–126. doi:10.1670/17.110
- Den Hartog, J., & Reijns, R. (2015). ‘I<sup>3</sup>S Straighten Manual, ver. 1.0.’ (Free Software Foundation: Boston, MA, USA.)
- Den Hartog, J., & Reijns, R. (2016). ‘I<sup>3</sup>S Pattern+ Manual, ver. 4.1.’ (Free Software Foundation: Boston, MA, USA.)
- Drechsler, A., Bock, D., Ortmann, D., and Steinfartz, S. (2010). Ortmann’s funnel trap: a highly efficient tool for monitoring amphibian species. *Herpetology Notes* **3**, 13–21.
- Dunbar, S. G., Ito, H. E., Bahjri, K., Dehom, S., and Salinas, L. (2014). Recognition of juvenile hawksbills *Eretmochelys imbricata* through face scale digitization and automated searching. *Endangered Species Research* **26**, 137–146. doi:10.3354/esr00637
- Ferner, J. W. (2010). Measuring and marking post-metamorphic amphibians. In ‘Amphibian Ecology and Conservation: A Handbook of Techniques’. (Ed. C. K. Dodd.) pp. 123–141. (Oxford University Press: Oxford, UK.)
- Gardner, W., Mulvey, E., and Shaw, E. (1995). Regression analyses of counts and rates: Poisson, overdispersed Poisson, and negative binomial models. *Psychological Bulletin* **118**(3), 392–404. doi:10.1037/0033-2909.118.3.392
- Glonek, G. F. V., and McCullagh, P. (1995). Multivariate logistic models. *Journal of the Royal Statistical Society. Series A* **57**, 533–546. doi:10.1111/j.2517-6161.1995.tb02046.x
- Hayes, C. T., Baumbach, D. S., Juma, D., and Dunbar, S. G. (2017). Impacts of recreational diving on hawksbill sea turtle (*Eretmochelys imbricata*) behaviour in a marine protected area. *Journal of Sustainable Tourism* **25**(1), 79–95. doi:10.1080/09669582.2016.1174246
- Jain, A. K. (2007). Biometric recognition. *Nature* **449**, 38–40. doi:10.1038/449038a
- Matos, C., Petrovan, S. O., Wheeler, P. M., and Ward, A. I. (2018). Short-term movements and behaviour govern the use of road mitigation measures by a protected amphibian. *Animal Conservation* **22**(3), 285–296. doi:10.1111/acv.12467

- Matthé, M., Sannolo, M., Winiarski, K., Spitzen-van der Sluijs, A., Goedbloed, D., Steinfartz, S., and Stachow, U. (2017). Comparison of photo-matching algorithms commonly used for photographic capture–recapture studies. *Ecology and Evolution* **7**(15), 5861–5872. doi:10.1002/ece3.3140
- Morrison, T. A., Keinath, D., Estes-Zumpf, W., Crall, J. P., and Stewart, C. V. (2016). Individual identification of the endangered wyoming toad *Anaxyrus baxteri* and implications for monitoring species recovery. *Journal of Herpetology* **50**, 44–49. doi:10.1670/14-155
- R Development Core Team (2018). 'R: a Language and Environment for Statistical Computing.' (R Foundation for Statistical Computing: Vienna, Austria.) Available at <http://www.R-project.org/> [verified 2 July 2020].
- Ribeiro, J., and Rebelo, R. (2011). Survival of *Alytes cisternasii* tadpoles in stream pools: a capture-recapture study using photo-identification. *Amphibia-Reptilia* **32**, 365–374. doi:10.1163/017353711X584186
- Sacchi, R., Scali, S., Mangiacotti, M., Sannolo, M., and Zuffi, M. A. L. (2016). Digital identification and analysis. In 'Reptile Ecology and Conservation. A Handbook of Techniques: (Ed. C. K. Dodd.) pp. 59–72. (Oxford University Press, Oxford, UK.)
- Sannolo, M., Gatti, F., Mangiacotti, M., Scali, S., and Sacchi, R. (2016). Photo-identification in amphibian studies: a test of I3S Pattern. *Acta Herpetologica* **11**, 63–68. doi:10.13128/Acta\_Herpetol-17198
- Sreekar, R., Purushotham, C. B., Saini, K., Rao, S. N., Pelletier, S., and Chaplod, S. (2013). Photographic capture–recapture sampling for assessing populations of the Indian gliding lizard *Draco dussumieri*. *PLoS One* **8**(2), e55935. doi:10.1371/journal.pone.0055935
- Steinmetz, K., Webster, I., Rowat, D., and Bluemel, J. K. (2018). Evaluating the software I3S Pattern for photo-identification of nesting hawksbill turtles (*Eretmochelys imbricata*). *Marine Turtle Newsletter* **155**, 15–19.
- Suriyamongkol, T., and Mali, I. (2018). Feasibility of using computer-assisted software for recognizing individual Rio Grande cooter (*Pseudemys gorzugi*). *Copeia* **106**(4), 646–651. doi:10.1643/CH-18-101
- Treilibs, C. E., Pavey, C. R., Hutchinson, M. N., and Bull, C. M. (2016). Photographic identification of individuals of a free-ranging, small terrestrial vertebrate. *Ecology and Evolution* **6**(3), 800–809. doi:10.1002/ece3.1883
- Van Tienhoven, A. M., Den Hartog, J. E., Reijns, R. A., and Peddemors, V. M. (2007). A computer-aided program for pattern-matching of natural marks on the spotted raggedtooth shark *Carcharias taurus*. *Journal of Applied Ecology* **44**, 273–280. doi:10.1111/j.1365-2664.2006.01273.x
- Venables, W. N., and Ripley, B. D. (2002). Random and mixed effects. In 'Modern Applied Statistics with S. Statistics and Computing'. (Eds. W. N. Venables, and B. D. Ripley.) pp. 271–300. (Springer: New York, NY, USA.)
- Ver Hoef, J. M., and Boveng, P. (2007). Quasi-Poisson vs. negative binomial regression: how should we model overdispersed count data? *Ecology* **88**, 2766–2772. doi:10.1890/07-0043.1
- Wessels, J. L., Carter, E. T., Hively, C. L., Hayter, L. E., and Fitzpatrick, B. M. (2018). Population viability of non-native Mediterranean house geckos (*Hemidactylus turcicus*) at an urban site near the northern invasion front. *Journal of Herpetology* **52**(2), 215–222. doi:10.1670/16-173

Handling Editor: Andrea Taylor